A Combined Gas-Phase, Solution-Phase, and Computational Study of C−H Activation by Cationic Iridium(III) Complexes

Christian Hinderling, Derek Feichtinger, Dietmar A. Plattner,* and Peter Chen*

Contribution from the Laboratorium für Organische Chemie der Eidgenössischen Technischen Hochschule (ETH) Zürich, CH-8092 Zürich, Switzerland

Received March 28, 1997[⊗]

Abstract: A combination of electrospray ionization MS/MS techniques, isotopic labeling experiments in the gas-phase and solution, and *ab initio* calculations is used to study the C−H activation reactions of $[Cp*Ir(PMe_3)(CH_3)]^+$ and $[CpIr(PMe_3)(CH_3)]^+$. The reaction in the gas phase was found to proceed through a Cp or $[Cp*Ir(\eta^2\text{-}CH_2\text{-}PMe_2)]^+$ intermediate. Quantitative collision-induced dissociation (CID) threshold measurements were used along with general models for ion−molecule reactions to construct potential energy diagrams which rationalize the gas-phase results. The comparison between the two complexes, and between the reactions in the gas phase and in solution, suggests that the reaction through the intermediacy of a metallaphosphacyclopropane could be favored over the conventional (and simpler) oxidative addition/reductive elimination mechanism when the Ir(III) complex is rendered more electron deficient.

Introduction

The chemical activation of alkane C−H bonds under mild conditions has been a long-standing goal in organic and organometallic chemistry.[1] Two mechanisms have been suggested by Bergman and co-workers[2,3] for the recently reported σ-bond metathesis reaction by cationic Ir(III) complexes,[4] cited as the most facile C−H activation reaction yet found for an organometallic complex (Scheme 1). Although one would ordinarily expect late transition metals to engage in an oxidative addition/reductive elimination sequence of reactions, the concerted mechanism comes into consideration for the Ir(III) complex because it might be unfavorable for the strongly electron-deficient 16-electron Ir(III) complex to go to an 18-electron Ir(V) species in an oxidative addition step. These complexes, extensively investigated recently by Bergman and co-workers,[2,3,5] perform C−H activation without prior photo-chemical excitation, and are therefore particularly interesting as model systems leading to catalytic cycles. On the basis of the increase in reactivity as the ligand binding is weakened, going from triflate to dichloromethane, the actual reactive species was presumed to be **2**, which would be formed from **1** in a pre-equilibrium in the solution-phase studies. For the dichloromethane-ligated complex, activation of C−H bonds was observed well below room temperature. According to *ab initio* calculations by Hall and co-workers,[6] an oxidative addition/reductive elimination mechanism is more likely than the concerted metathesis, although solid experimental evidence for either alternative has yet to be presented. A similar pattern of reactivity, with the same set of mechanistic possibilities, has also been reported for Pt(II) complexes.[7]

Scheme 1

two-step addition-elimination mechanism

concerted σ-bond metathesis mechanism
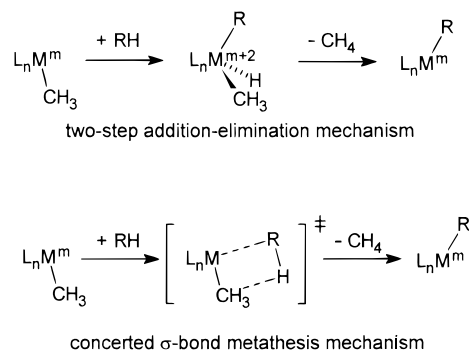
We report here experimental and computational results which clearly demonstrate that the C−H activation reaction by cationic Ir(III) complexes like **2** and **6**, in the gas phase, proceeds by a third mechanism, namely, the elimination of CH_4 to produce an intermediate metallaphosphacyclopropane, and then, ultimately, reaction with the C−H bond of alkanes and arenes (Scheme 2). A preliminary report of the gas-phase chemistry of organometallic ions **5**−**8** (Scheme 3) by electrospray tandem mass spectrometry has recently appeared.[8] We expand and complement that work in the present report with an extension of the study to the complexes **1**−**4**, solution-phase isotopic labeling experiments, *ab initio* quantum chemical calculations, and quantitative collision-induced dissociation (CID) threshold measurements. The comparison of the Cp and Cp* series of complexes, as well as the comparison of gas-phase to solution-phase reactivity, illuminates the features determining the choice between competing mechanisms for C−H activation.

Experimental Section

Preparation of the organometallic complexes in this study was done by standard Schlenk techniques or in an argon-purged glovebox. Characterization of the compounds by ¹H and ¹³C NMR (Varian GEMINI 2000, 300 MHz), X-ray crystallography (Enraf Nonius Mach 3), and electrospray mass spectrometry (Finnigan MAT TSQ-7000) was done. Detailed synthetic procedures for the various complexes, their

⊗ Abstract published in *Advance ACS Abstracts,* October 15, 1997.

(1) Arndtsen, B. A.; Bergman, R. G.; Mobley, T. A.; Petersen, T. H. *Acc. Chem. Res.* **1995**, *28*, 154.

(2) Arndtsen, B. A.; Bergman, R. G. *Science* **1995**, *270*, 1970.

(3) Burger, P.; Bergman, R. G. *J. Am. Chem. Soc.* **1993**, *115*, 10462.

(4) Recent progress in C−H activation by Ir(III) complexes has been reviewed: Lohrenz, J. C. W.; Jacobsen, H. *Angew. Chem.* **1996**, *108*, 1403; *Angew. Chem., Int. Ed. Engl.* **1996**, *35*, 1305.
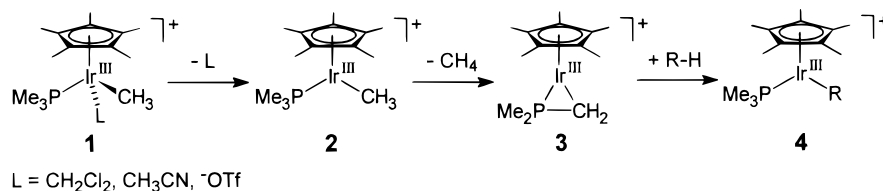
(5) Veltheer, J. E.; Burger, P.; Bergman, R. G. *J. Am. Chem. Soc.* **1995**, *117*, 12478.

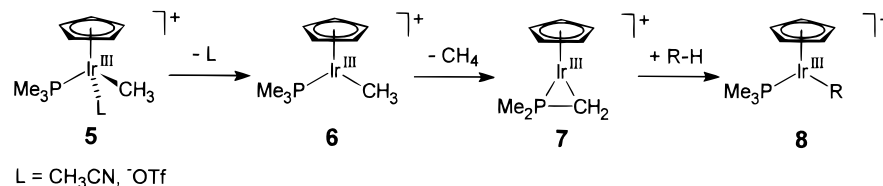(6) Strout, D. L.; Zaric, S.; Niu, S.; Hall, M. B. *J. Am. Chem. Soc.* **1996**, *118*, 6068.

(7) Holtcamp, M. W.; Labinger, J. A.; Bercaw, J. E. *J. Am. Chem. Soc.* **1997**, *119*, 848.

(8) Hinderling, C.; Plattner, D. A.; Chen, P. *Angew. Chem.* **1997**, *109*, 272; *Angew. Chem., Int. Ed. Engl.* **1997**, *36*, 243.

Scheme 2

Me_3P···Ir^{III}(CH_3)(L) $\xrightarrow{-\text{L}}$ Me_3P–Ir^{III}(CH_3) $\xrightarrow{-\text{CH}_4}$ Me_2P–CH_2 Ir^{III} $\xrightarrow{+\text{R-H}}$ Me_3P–Ir^{III}(R)

1   **2**   **3**   **4**

L = CH_2Cl_2, CH_3CN, ⁻OTf

Scheme 3

Me_3P···Ir^{III}(CH_3)(L) $\xrightarrow{-\text{L}}$ Me_3P–Ir^{III}(CH_3) $\xrightarrow{-\text{CH}_4}$ Me_2P–CH_2 Ir^{III} $\xrightarrow{+\text{R-H}}$ Me_3P–Ir^{III}(R)

5   **6**   **7**   **8**

L = CH_3CN, ⁻OTf

physical characterization, and the procedures by which the solution-phase reactions were done are given in the Supplemental Information.

Complexes **1** (L = ⁻OTf, CH_3CN) were prepared according to the procedures by Burger and Bergman,[3] starting from the dimeric complex,[9] [Cp*Ir(Cl)_2]_2, and proceeding through the equilibration of the bis-methyl complex,[10] Cp*Ir(PMe_3)(CH_3)_2, with the bis-triflate,[11] Cp*Ir(PMe_3)(OTf)_2. Complexes **5** (L = ⁻OTf, CH_3CN) were prepared analogously,[8] starting from CpIr(C_2H_4)_2, described by Heinekey,[12] which was converted to the polymeric complex [CpIr(Cl)_2]_n (not isolated), and then taken on to **5** as detailed in the Supplemental Information.

Cations **2** and **6**, the [Cp*Ir(PMe_3)(CH_3)]^+ and [CpIr(PMe_3)(CH_3)]^+ complexes, were prepared in the gas phase by electrospray of CH_2Cl_2 or $CHCl_3$ solutions containing the [Cp*Ir(PMe_3)(CH_3)]^+ or the [CpIr-(PMe_3)(CH_3)]^+ cations. The slightly modified Finnigan MAT TSQ7000 electrospray tandem mass spectrometer was set up with an octopole, quadrupole, octopole, quadrupole (O1/Q1/O2/Q2) configuration behind a conventional electrospray ion source.[13] The extent of desolvation and collisional activation prior to thermalization, reaction, and/or analysis was controlled by the tube lens potential in the electrospray source, which typically ranged from 35 (mild conditions) to 75 V (hard conditions).[14] The first octopole was fitted with an open cylindrical sheath around the rods into which a collision gas could be bled for thermalization or reaction at pressures up to 20 mTorr. Control experiments with Mn(CO)_6^+ have found that ~10 mTorr of Ar in O1 are sufficient[15] for thermalization of ions produced by the electrospray source to the 70 °C manifold temperature. It should be noted here that heating of the external inlet lines for the thermalization gas is important to ensure that the gas is fully equilibrated to the manifold temperature. The second octopole was operated as a conventional collision-induced dissociation (CID) cell, and run as specified in the commercial instrument for MS/MS experiments. Spectra were recorded in three different modes. In the normal ES-MS mode, only one quadrupole is operated, and an ordinary mass spectrum of the electrosprayed ions is recorded. This mode, exemplified by entries 1−3 and 13−18 in Table 1, serves primarily to characterize the ions produced by a given set of conditions. In the daughter-ion mode, used in entries 4−12 and 19−22 in Table 1, Q1 is used to mass-select ions

of a single mass from among all of the ions produced in O1, which are then collided or reacted with a target gas in O2, and mass-analyzed by Q2. This mode is used to determine the specific reactivity of a species of a given mass. The third mode of operation, the RFD mode, is used to record CID thresholds for quantitative thermochemical measurements.[16,17] Ions produced in O1 are again mass-selected, but with Q1 acting as a high-pass filter. The selected ions are then collided with a target gas in O2, and mass-analyzed in Q2. In the RFD mode, the reactions of ions in a particular mass range are isolated by setting the mass cutoff above and below the desired range and subtracting the latter from the former spectra. The more complicated RFD mode operation is used instead of the daughter-ion mode for the threshold measurements because the ion kinetic energy distribution is narrower (~0.4−0.6 versus ~1.3−2.0 eV fwhm in the laboratory frame). Furthermore, the kinetic energy distribution in the RFD mode is nearly Gaussian, in comparison to a distribution in daughter-ion mode that, while also not too far from Gaussian, has a non-negligible high-energy tail. Both factors combine to make deconvolution of the threshold measurement more reliable (even though we can use the measured kinetic energy distribution in the fit). *In both the daughter-ion and RFD modes (unless otherwise specified), the pressure in O2 was kept low enough so as to minimize the chance of multiple collisions in the collision cell.*[18] A kinetic energy distribution of the ions in the laboratory frame of <0.6 eV fwhm corresponds to a distribution of <0.1 eV in the center-of-mass frame when the collision partner is argon or xenon, and is a non-negligible contributor to the cited ±2 kcal/mol uncertainty in the CID threshold determinations. As a control to check that we could correctly measure CID thresholds, we reproduced experiments by Kebarle[19] and Armentrout[20,21] for the reaction (H_2O)_n-(H_3O^+) → (H_2O)_{n-1}(H_3O^+) + H_2O. The threshold for n = 1 was

(9) White, C.; Yates, A.; Maitlis, P. M. *Inorg. Syn.* **1992**, *29*, 228.

(10) Buchanan, J. M.; Stryker, J. M.; Bergman, R. G. *J. Am. Chem. Soc.* **1986**, *108*, 1537.

(11) Stang, P. J.; Huang, Y.; Arif, A. M. *Organometallics* **1992**, *11*, 231.

(12) Heinekey, D. M.; Miller, J. M.; Koetzle, T. F.; Payne, N. G.; Zilm, K. W. *J. Am. Chem. Soc.* **1990**, *112*, 909.

(13) The basic electrospray source for mass spectrometry is described by: Whitehouse, C. M.; Dreyer, R. N.; Yamashita, M.; Fenn, J. B. *Anal. Chem.* **1985**, *57*, 675.

(14) Approximate ranges for tube lens potentials are the following: low ≈30−44 V, medium ≈45−60 V, high ≈60−80 V.

(15) Thermalization was judged to be complete when an observed (but relatively weak) dependence of the CID threshold curves for the loss of one CO ligand on the temperature of the heated capillary (from 100 to 240 °C) in the electrospray ion source was eliminated. N_2 in the sheath gas was found to give a small amount of a dinitrogen complex with the 16-electron complexes. For mass spectra in the "normal" mode, CO_2 was therefore used as the sheath gas. For daughter-ion and RFD modes, in which there is a mass-selection step in the experiment, N_2 could be used.

(16) The present state of organometallic thermochemistry for Ir complexes is reviewed by: Halpern, J. *Inorg. Chim. Acta* **1985**, *100*, 41. In particular, Stoutland et al. (Stoutland, P. O.; Bergman, R. G.; Nolan, S. P.; Hoff, C. D.; *Polyhedron* **1988**, *7*, 1429) find reasonably certain Ir−H and Ir−C bond strengths for (Cp*)(PMe_3)Ir(cyclohexyl)(H) of 75 and 52 kcal/mol, respectively.

(17) Thermochemical work by mass spectrometric techniques has been done for small organometallic ions. For several examples, see: Halle, L. F.; Armentrout, P. B.; Beauchamp, J. L. *Organometallics* **1982**, *1*, 963. Armentrout, P. B.; Halle, L. F.; Beauchamp, J. L. *J. Am. Chem. Soc.* **1981**, *103*, 6501. Armentrout, P. B.; Beauchamp, J. L. *J. Am. Chem. Soc.* **1981**, *103*, 784. For some more recent work on small complexes, see: Sunderlin, L. S.; Wang, D.; Squires, R. R. *J. Am. Chem. Soc.* **1993**, *115*, 12060. Sunderlin, L. S.; Squires, R. R. *J. Am. Chem. Soc.* **1993**, *115*, 337.

(18) Pressure in the collision cell was kept below 4 × 10^{-5} torr (usually argon), as measured by a cold cathode gauge. The interaction region was 18.5 cm long. Typically, thresholds were measured at four different pressures and extrapolated to zero pressure. Even at the highest pressures used, the amount of fragmentation of the parent ions remained below 15%.

(19) Anderson, S. G.; Blades, A. T.; Klassen, J.; Kebarle, P. *Int. J. Mass Spectrom. Ion Proc.* **1995**, *141*, 217. We observed the threshold for loss of H_2O from protonated water dimer to be E_0 = 1.28 eV (298 K value). The absolute value of the energy scale was determined by stepping the potential of the collision cell, and then fitting the derivative of the resulting retardation curve to a Gaussian function. The maximum of the Gaussian was taken as the absolute zero of the energy scale. It coincided with the potential of the first octopole.

Table 1. Schematic Description of the Gas-Phase Tandem Mass Spectrometric Experiments on Complexes **1** and **5**[a]

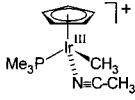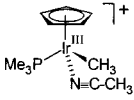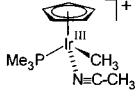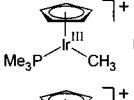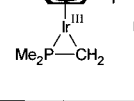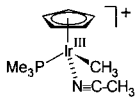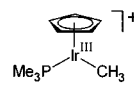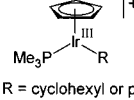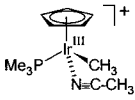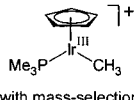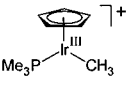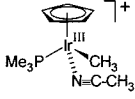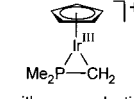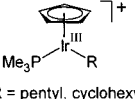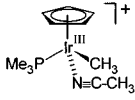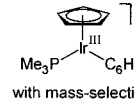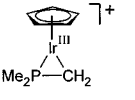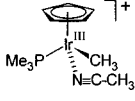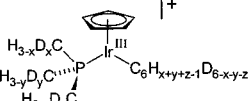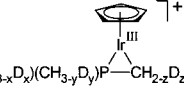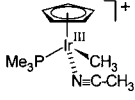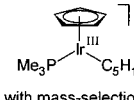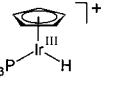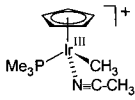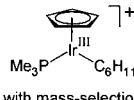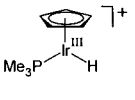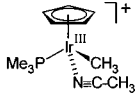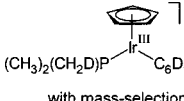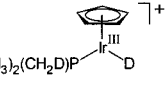|	Precursor:	is electrosprayed into Q1 where there is:	producing in Q1:	which is collided in Q2 with:	producing in Q2:	Comments:
1	[structure: Cp*Ir(PMe3)(CH3)(N≡C-CH3)]+ ClO4-	10 mTorr CO2 / low tube lens potential	[structure: Cp*Ir(PMe3)(CH3)(N≡C-CH3)]+	----	----	production of intact molecular ions
2	[structure: Cp*Ir(PMe3)(CH3)(N≡C-CH3)]+ ClO4-	10 mTorr CO2 / higher tube lens potential	[structure: Cp*Ir(PMe3)(CH3)]+ major; [structure: Cp*Ir(Me2P—CH2)]+ minor	----	----	collisional removal of the most weakly bound ligand
3	[structure: Cp*Ir(PMe3)(CH3)(N≡C-CH3)]+ ClO4-	10 mTorr of Ar / 10 mTorr cyclohexane or benzene / the higher tube lens potential	[structure: Cp*Ir(PMe3)(CH3)]+ major; [structure: Cp*Ir(PMe3)(R)]+ minor, R = cyclohexyl or phenyl	----	----	amount of adduct corresponds to the amount of cyclic ion in the previous experiment
4	[structure: Cp*Ir(PMe3)(CH3)(N≡C-CH3)]+ ClO4-	10 mTorr N2 / the higher tube lens potential	[structure: Cp*Ir(PMe3)(CH3)]+ with mass-selection to exclude other ions	pentane or benzene	[structure: Cp*Ir(PMe3)(CH3)]+	no reaction in Q2 until collision energies are high enough to induce methane loss first
5	[structure: Cp*Ir(PMe3)(CH3)(N≡C-CH3)]+ ClO4-	10 mTorr N2 / high tube lens potential	[structure: Cp*Ir(Me2P—CH2)]+ with mass-selection to exclude other ions	pentane or benzene	[structure: Cp*Ir(PMe3)(R)]+ R = pentyl, cyclohexyl, or phenyl	even at the lowest available collision energies
6	[structure: Cp*Ir(PMe3)(CH3)(N≡C-CH3)]+ ClO4-	10 mTorr CO2 / 10 mTorr C6H6 / high tube lens potential	[structure: Cp*Ir(PMe3)(C6H5)]+ with mass-selection to exclude other ions	xenon	[structure: Cp*Ir(Me2P—CH2)]+	addition of benzene to the cyclic ion is reversible at modest collision energies
7	[structure: Cp*Ir(PMe3)(CH3)(N≡C-CH3)]+ ClO4-	10 mTorr CO2 / 10 mTorr C6D6 / high tube lens potential	[structure: Cp*Ir[(H3-xDxC)(H3-yDyC)(H3-zDzC)P](C6Hx+y+z-1D6-x-y-z)]+ with x+y+z ≤ 6 and mass selection to exclude other ions	xenon	[structure: Cp*Ir[(CH3-xDx)(CH3-yDy)P—CH2-zDz]]+ with x ≤ 3, y ≤ 3, z ≤ 2 and x+y+z ≤ 6	up to 6 deuteriums remain after loss of benzene upon CID
8	[structure: Cp*Ir(PMe3)(CH3)(N≡C-CH3)]+ ClO4-	10 mTorr CO2 / 10 mTorr n-C5H12 / high tube lens potential	[structure: Cp*Ir(PMe3)(C5H11)]+ with mass-selection to exclude other ions	xenon	[structure: Cp*Ir(PMe3)(H)]+	loss of pentene upon CID
9	[structure: Cp*Ir(PMe3)(CH3)(N≡C-CH3)]+ ClO4-	10 mTorr CO2 / 10 mTorr c-C6H12 / high tube lens potential	[structure: Cp*Ir(PMe3)(C6H11)]+ with mass-selection to exclude other ions	xenon	[structure: Cp*Ir(PMe3)(H)]+	loss of cyclohexene upon CID
10	[structure: Cp*Ir(PMe3)(CH3)(N≡C-CH3)]+ ClO4-	10 mTorr CO2 / 10 mTorr c-C6D12 / high tube lens potential	[structure: Cp*Ir[(CH3)2(CH2D)P](C6D11)]+ with mass-selection to exclude other ions	xenon	[structure: Cp*Ir[(CH3)2(CH2D)P](D)]+	loss of cyclohexene upon CID with 2 deuterium remaining on the complex

Table 1. (Continued)
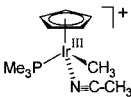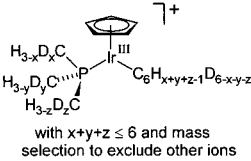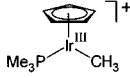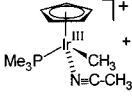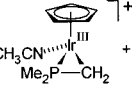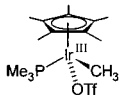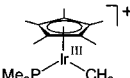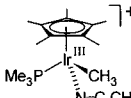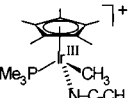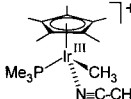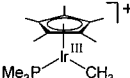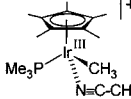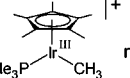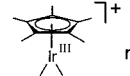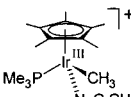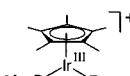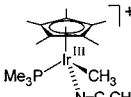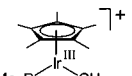
	Precursor:	is electrosprayed into O1 where there is:	producing in Q1:	which is collided in O2 with:	producing in Q2:	Comments:
11		10 mTorr CO_2 / 10 mTorr C_6D_6 / high tube lens potential	with x+y+z ≤ 6 and mass selection to exclude other ions	xenon / very high collision energies		multiple products but the $[CpIr]^+$ fragment contained no deuteriums
12		10 mTorr Ar / high enough tube lens potential to remove acetonitrile ligand	with mass-selection to exclude other ions	CH_3CN / low collision energy	**+ 6** **+ 7**	(**6** + CH_3CN) / **6** / (**7** + CH_3CN) / **7** in ratio 100 / 5 / 12 / 3. The 16-e⁻ complexes readily bind a 2-e⁻ ligand like acetonitrile. Very similar results with CO
13		10 mTorr N_2 / low tube lens potential		----	----	in solution, the triflate is partially ionized, so it can be electrosprayed directly
14		10 mTorr CO_2 / low tube lens potential		----	----	results analogous to the Cp complex
15		10 mTorr CO_2 / slightly higher tube lens potential		----	----	facile loss of the weakly bound acetonitrile ligand
16		10 mTorr CO_2 / high tube lens potential	**minor** **major**	----	----	collisional activation causes loss of methane and predominant formation of the cyclic complex
17		10 mTorr CO_2 / 10 mTorr pentane or benzene / high tube lens potential	R = pentyl or phenyl	----	----	reactions identical to those in the Cp complex except that the Cp* complex did not react with cyclohexane
18		10 mTorr CO_2 / 10 mTorr C_6D_6 / high tube lens potential		----	----	the presence of benzene in the O1 leads to the disappearance of the cyclic ion and the appearance of the benzene adduct
19		10 mTorr N_2 / 10 mTorr n-C_5H_{12} / high tube lens potential	with mass-selection to exclude other ions	xenon		loss of pentene upon CID

Table 1. (Continued)

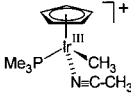| Precursor:	is electrosprayed into O1 where there is:	producing in Q1:	which is collided in O2 with:	producing in Q2:	Comments:
20 [Cp*Ir(III)(Me$_3$P)(CH$_3$)(N≡C–CH$_3$)]$^+$ $^-$OTf	10 mTorr CO$_2$ / 10 mTorr C$_6$D$_6$ / high tube lens potential	[Cp*Ir(III)((CH$_3$)$_2$(CH$_2$D)P)(C$_6$D$_5$)]$^+$ with mass-selection to exclude other ions	xenon	[Cp*Ir(III)((CH$_3$)(CH$_{3-x}$D$_x$)P)(CH$_{2-y}$D$_y$)]$^+$ with x+y ≤ 1	loss of benzene upon CID with either 0 or 1 deuterium remaining on the cyclic complex
21 [Cp*Ir(III)((CD$_3$)$_3$P)(CH$_3$)(N≡C–CH$_3$)]$^+$ $^-$OTf	10 mTorr N$_2$ / high tube lens potential	[Cp*Ir(III)((CD$_3$)$_2$P–CD$_2$)]$^+$	----	----	the mass of the ion clearly indicates that CH$_3$D was lost upon CID
22 [Cp*Ir(III)((CD$_3$)$_3$P)(CH$_3$)(N≡C–CH$_3$)]$^+$ $^-$OTf	10 mTorr N$_2$ / high tube lens potential	[Cp*Ir(III)((CD$_3$)$_2$P–CD$_2$)]$^+$ with mass-selection to exclude other ions	C$_6$H$_6$	[Cp*Ir(III)((CD$_3$)$_2$(CHD$_2$)P)(C$_6$H$_5$)]$^+$	some scrambling of the isotope labels is evident at much higher collision energies

[a] Entries without items in O2 and Q2 are ordinary electrospray mass spectra. Items with the designation "mass selection..." indicate daughter-ion spectra.

extracted from our data with Armentrout's CRUNCH program, yielding a value in agreement with the published data.[19,21]

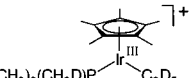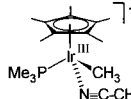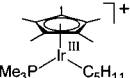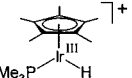*Ab initio* calculations of geometries and frequencies for the organometallic complexes in this report were performed with Gaussian 94[22] on IBM RS/6000-590 or DEC Alpha AXP 8400 5/300 workstations. The initial calculations at the Hartree–Fock level employed a basis set comprising the Hay and Wadt effective core potential[23] (ECP) for iridium and a modest 3-21G basis set for the light atoms, comparable to that found by Frenking and co-workers,[24] to give good geometries and relative energies for other organometallic systems. The larger LANL2DZ basis set[22] (D95 on first row, Los Alamos ECP plus double-ζ on Na-Bi) was used for subsequent Hartree–Fock and DFT (with the B3LYP density functional) calculations. Full geometry optimization and frequency calculation was done at the Hartree–Fock level and with DFT, yielding very similar results throughout. The DFT calculations closely parallel those by Hall,[6] and by Siegbahn,[25] for other metal systems. The consistency of the geometries at differing levels of theory and their intuitive reasonableness lend credibility to the computational results. Accordingly, the DFT calculations with the large basis were deemed sufficient for the computation of frequencies to be used in the RRKM kinetic shift calculations needed to extract thermochemistry from CID threshold measurements. Even at this relatively modest level of theory, the computation of sufficiently realistic geometries and frequencies represents one of the real-life limiting factors in the entire experiment.

Results

The gas-phase results are summarized in Table 1. Some representative mass spectra, keyed to the table entries, are shown

(20) Dalleska, N. F.; Honma, K.; Armentrout, P. B. *J. Chem. Phys.* **1989**, *90*, 5466.

(21) Dalleska, N. F.; Honma, K.; Armentrout, P. B. *J. Am. Chem. Soc.* **1993**, *115*, 12125.

(22) *Gaussian 94* (Revision A.1); M. J. Frisch, G. W. Trucks, H. B. Schlegel, P. M. W. Gill, B. G. Johnson, M. A. Robb, J. R. Cheeseman, T. A. Keith, G. A. Petersson, J. A. Montgomery, K. Raghavachari, M. A. Al-Laham, V. G. Zakrzewski, J. V. Ortiz, J. B. Foresman, J. Cioslowski, B. J. Stefanov, A. Nanyakkara, M. Challacombe, C. Y. Peng, P. Y. Ayala, W. Chen, M. W. Wong, J. L. Andres, E. S. Replogle, R. Gomperts, R. L. Martin, D. J. Fox, J. S. Binkley, D. J. DeFrees, J. Baker, J. P. Stewart, M. Head-Gordon, C. Gonzalez, and J. A. Pople; Gaussian, Inc.: Pittsburgh, PA, 1995.

(23) Hay, R. J.; Wadt, W. R. *J. Chem. Phys.* **1985**, *82*, 270, 284, 299.

(24) Jonas, V.; Frenking, G.; Reetz, M. T. *J. Comp. Chem.* **1992**, *13*, 919. Jonas, V.; Frenking, G.; Reetz, M. T. *J. Comp. Chem.* **1992**, *13*, 935. Veldkamp, A.; Frenking, G. *J. Comp. Chem.* **1992**, *13*, 1184.

(25) Siegbahn, P. E. M. *J. Am. Chem. Soc.* **1996**, *118*, 1487.
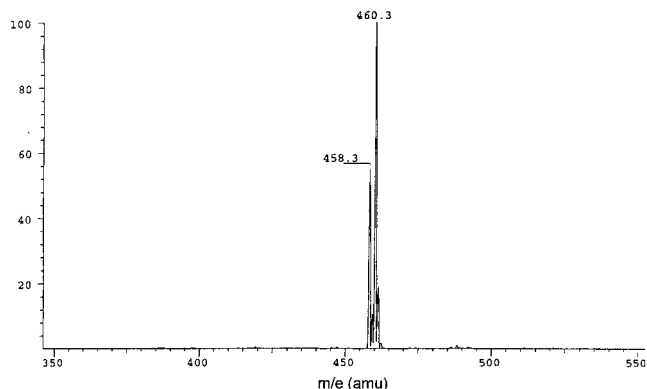
Figure 1. Electrospray mass spectrum of [Cp*Ir(PMe$_3$)(CH$_3$)-(N≡CCH$_3$)]$^+$ with the *m/e* 458, 460 doublet due to the 1:2 natural abundance of [191]Ir and [193]Ir, taken with a very low tube lens potential, showing the intact organometallic molecular ion transferred from solution to the gas phase. The spectrum corresponds to entry 14 in Table 1.
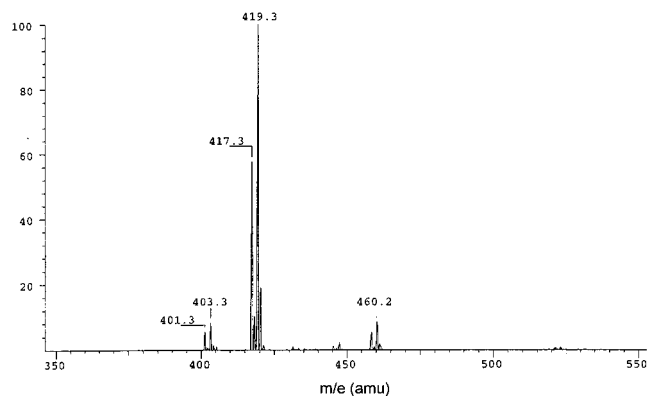
Figure 2. Electrospray mass spectrum of [Cp*Ir(PMe$_3$)(CH$_3$)]$^+$ with the *m/e* 417, 419 doublet due to the 1:2 natural abundance of [191]Ir and [193]Ir, taken with the application of a larger tube lens potential to remove the weakly bound solvent ligand. The spectrum corresponds to entry 15 in Table 1.

in Figures 1–6 to illustrate the quality of the original data. With some small differences (indicated below), the reactions of the [Cp*Ir(PMe$_3$)(CH$_3$)]$^+$ and [CpIr(PMe$_3$)(CH$_3$)]$^+$ complexes **2** and
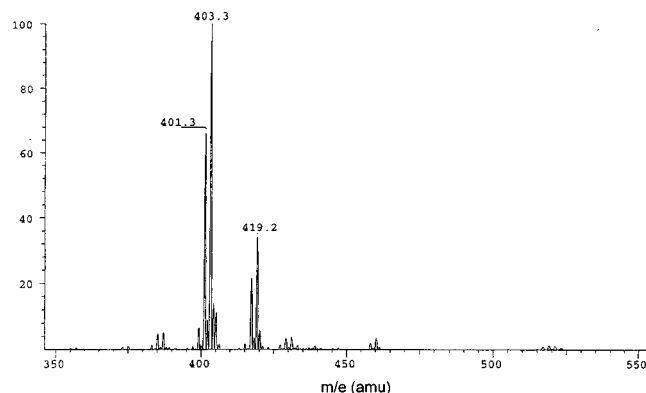
Figure 3. Electrospray mass spectrum of cyclic cation, [Cp*Ir(η^2-(CH$_2$PMe$_2$)]$^+$, with the *m/e* 401, 403 doublet due to the 1:2 natural abundance of ^{191}Ir and ^{193}Ir, taken with the application of a high enough tube lens potential to induce the elimination of CH$_4$ by CID. The spectrum corresponds to entry 16 in Table 1.
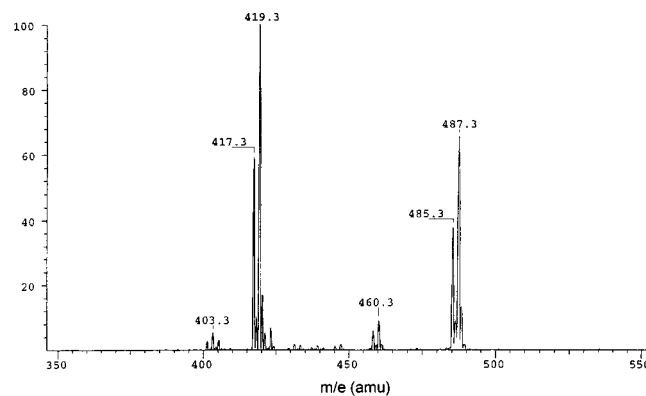

Figure 4. Electrospray mass spectrum of [Cp*Ir(PMe$_3$)(CH$_3$)]$^+$ at *m/e* 417, 419 and [Cp*Ir(PMe$_3$)(Ph)]$^+$-d_6 at *m/e* 485, 487, prepared by reaction of a mixture (such as shown in Figure 3) of [Cp*Ir(PMe$_3$)(CH$_3$)]$^+$ and [Cp*Ir(η^2-CH$_2$PMe$_2$)]$^+$ with benzene-d_6. The spectrum corresponds to entry 18 in Table 1.

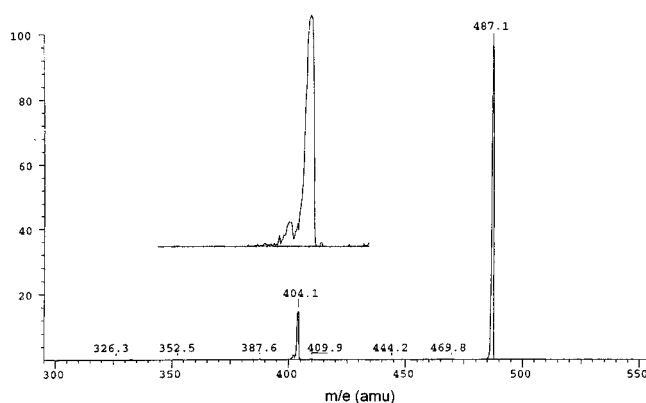**Figure 5.** Electrospray mass spectrum, in daughter-ion mode, of the products from the collision-induced dissociation of mass-selected [Cp*Ir(PMe$_3$)(Ph)]$^+$-d^6 (only the ^{193}Ir isotopic species) with xenon as the collision partner. The peaks at *m/e* 404 and 487 correspond to the ion with and without loss of benzene-d_5. The expanded inset showing the *m/e* 404 peak also shows a small peak at *m/e* 403, corresponding to loss of benzene-d_6 upon CID. The spectrum corresponds to entry 20 in Table 1.

6 are entirely parallel, with the Cp series of complexes showing qualitatively higher reactivity than their Cp* analogs. One can draw a series of broad conclusions from the observed gas-phase reactions.

(1) Electrospray ionization cleanly produces the molecular ion of organometallic complexes, with even weakly-bound ligands still intact [Table 1, entries 1, 13, and 14].
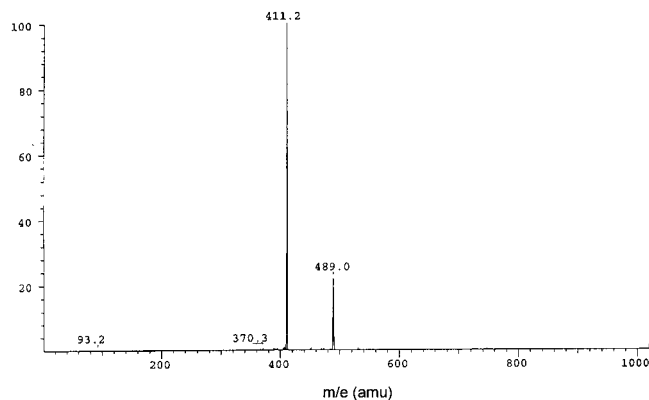

Figure 6. Electrospray mass spectrum, in daughter-ion mode, of the products from the gas-phase reaction of mass-selected [Cp*Ir(η^2-CD$_2$PMe$_2$-d_6)]$^+$ (only the ^{193}Ir isotopic species) and benzene. The peaks at *m/e* 411 and 489 correspond to the ion without and with addition of benzene. The spectrum corresponds to entry 22 in Table 1.

(2) The ion assigned as **6**, prepared by collisional removal of CH$_3$CN from **5** and thermalized, picks up neutral 2-e$^-$ ligands such as acetonitrile or CO with high efficiency at very low collision energies. Also evident (at much lower intensity) are the ions due to **7** and (**7** + acetonitrile) [Table 1, entry 12].

(3) After collisional removal of the acetonitrile ligand from **1** or **5**, the resulting ions **2** and **6** readily lose CH$_4$ with cyclometalation upon further CID [Table 1, entries 2, 5, 16, and 21].

(4) In the gas phase, all detectable cyclometalation proceeds exclusively on the methyl groups of the phosphine, and not on the Cp or Cp* [Table 1, entries 11 and 21].

(5) The metallaphosphacyclopropanes **3** and **7** react readily with pentane and benzene to yield the products (with respect to the original **2** and **6**) of an overall σ-bond metathesis [Table 1, entries 5 and 22].

(6) The addition of **3** or **7** to benzene is reversible upon further CID [Table 1, entries 6, 7, and 20].

(7) When β-hydride elimination is possible from **4** or **8**, it occurs upon CID [Table 1, entries 8, 9, and 19].

(8) The cyclometalated ions **3** and **7** are much more reactive, with regard to C−H activation in the gas phase, than the precursor ions **2** and **6** [Table 1, entries 3, 4, and 18].

The differences in the gas-phase chemistry of the Cp* complexes **1**−**4** and the Cp analogs **5**−**8** are confined to two areas. Comparing entry 3 or 5 to entry 17, one sees that, while the Cp-substituted complexes add to pentane, cyclohexane, or benzene, the Cp*-substituted analogs react with pentane or benzene only. No cyclohexane adducts were observed in the gas-phase reactions of **2** or **3**. Secondly, comparison of entries 7 and 19 shows that, in the CID of the two phenyl-substituted complexes **4** and **8** (R = Ph), there is complete deuterium scrambling in **8**, but only partial scrambling in **4**. An explanation for both observations, based on general features of ion−molecule reactions, will be given below in the Discussion. It should also be noted that reactions of **7** with methane produced only the barest hint of addition products.

The quantitative CID threshold (argon as collision partner) for loss of CH$_4$ from **6** to form **7** is shown, with the fit to an analytical threshold function, in Figure 7. The data were recorded as described in the RFD mode, and deconvoluted with the CRUNCH program from Armentrout and co-workers,[20,21] with the internal energy of the ions set by the 70 °C manifold temperature to which they were thermalized. The RRKM calculation comprising part of the deconvolution requires the frequencies for the product ions, as well as estimates for the five normal modes in the transition state that become, at the
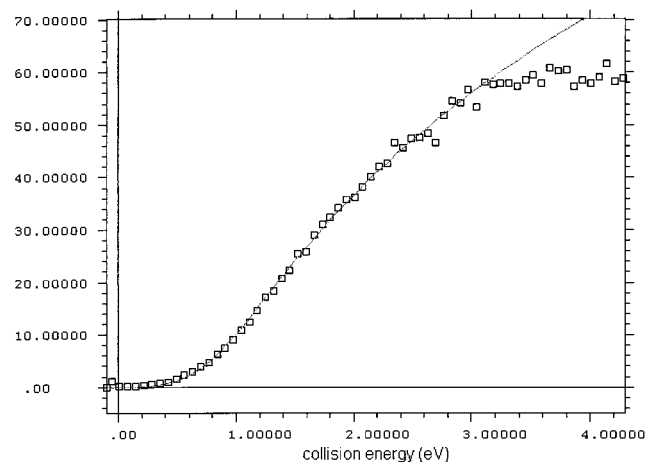
Figure 7. Representative collision-induced dissociation (CID) threshold curve for the reaction **6** → **7** + CH₄, showing the dependence of the dissociation cross-section (σ, 10^{-16} cm²) again collision energy (eV, center-of-mass frame), and the fit to Armentrout's threshold function (described in ref 17). The fit covered data between 0 and 3 eV, and yielded the following parameters (0 K): $E_0 = 0.58(2)$ eV, $\sigma = 52.8(3)$, and $n = 1.42(4)$.

asymptotic limit of dissociation, two translations and three rotations of the two departing fragments.[26] Numerical estimates for these five frequencies were taken from computations of analogous oxidative addition,[6] reductive elimination,[27] and σ-bond metathesis[28] transition states. Fortunately, the cyclic transition states for all of these chemical processes are relatively tight, showing for the desired modes similar frequencies. With use of 80, 135, 540, 1285, and 2050 cm⁻¹ for the five transition-state frequencies,[29] (anything over ~200 cm⁻¹ makes very little difference anyways), the deconvoluted threshold for the **6** → **7** + CH₄ reaction, corrected to 0 K, is $E_0 = 0.72 \pm 0.10$ eV, if all the vibrations are treated as harmonic. If a physically more realistic model is used in which the methyl groups, the phosphine as a whole, and the Cp ligand are treated as internal rotors,[30] then the deconvoluted threshold drops to $E_0 = 0.59 \pm 0.10$ eV, or 13.6 ± 2 kcal/mol (2σ error bounds). The drop in the deconvoluted threshold upon inclusion of internal rotations in the fit is expected because, in going from **6** to any of the conceivable transition states for methane loss, free rotation about two of the four methyl rotors, and the phosphine as well, is

(26) This methodology is described in: Loh, S. K.; Hales, D. A.; Lian, L.; Armentrout, P. B. *J. Chem. Phys.* **1989**, *90*, 5467.

(27) Obara, S.; Kitaura, K.; Morokuma, K. *J. Am. Chem. Soc.* **1984**, *106*, 7482.

(28) Rappé, A. K.; Upton, T. H. *J. Am. Chem. Soc.* **1992**, *114*, 7507. The transition state geometries for the Cl₂M(CH₃)(H)(CH₃) (M = Al, Sc) were reoptimized at the CAS(4,4)/LANL1DZ level. Frequencies at this level were then computed and used to guide the estimates for the current system.

(29) These frequencies came from the calculation described in ref 28. An alternative set of five frequencies taken from the calculation in ref 6 (149, 184, 488, 499, and 2243 cm⁻¹) produced deconvoluted thresholds that differed by *much* less than the stated ±0.1 eV error bounds.

(30) The internal rotor energy levels were computed from the reduced moments of inertia for rotation of the Cp ligand, the trimethylphosphine unit as a whole, and the individual methyl groups, using the computed equilibrium geometry of **6**. See: Berry, R. S.; Rice, S. A.; Ross, J. *Physical Chemistry*, 1st ed.; John Wiley: New York, 1980; p 771. Two methyl rotors, and rotation of the phosphine unit, are lost at the transition state, which accounts for the marked effect on the computed threshold energy.

(31) The dimeric nature of the complex is unambiguous from the isotope peaks in the mass spectrum. Because the ¹H NMR spectrum for the dimeric complex shows a single Cp resonance with no new splittings, and two different aliphatic peaks split by coupling to the phosphorus, both of which disappear in the dimer derived from the complex with a deuterated trimethylphosphine, one can place some constraints on the structure of the complex. Moreover, it is clear from the mass alone that methane loss has occurred. While a final judgment awaits further work, we believe the structure has a six-membered ring analogous to that found by X-ray crystallography for the dimer of (dmpe)₂Ru, characterized by: Cotton, F. A.; Frenz, B. A.; Hunter, D. L. *J. Chem. Soc., Chem. Commun.* **1974**, 755.

lost. The reported threshold is the average of five independent determinations. For each determination, four separate threshold measurements were done. A similar measurement for the **2** → **3** + CH₄ reaction was not attempted because the five additional methyl rotors on the Cp* ligand would result in a much larger kinetic shift, already ~0.4 eV in the reaction with **6**, making accurate determination of the threshold more difficult.

The solution-phase experiments showed somewhat different chemistry. Starting with the undeuterated complex [Cp*Ir-(PMe₃)(CH₃)(OTf)] in CD₂Cl₂, reaction with benzene-d_6 through the putative intermediacy of [Cp*Ir(η^2-CH₂PMe₂)]⁺, complex **3**, should lead to deuterium incorporation in the phosphine ligand and loss of CH₄ instead of CH₃D (Scheme 4). The mirror-image of the deuterium "wash-in" experiment would be a deuterium "wash-out" from [Cp*Ir(PMe₃-d_9)(CH₃)(OTf)] by reaction with C₆H₆ in CD₂Cl₂ solution. In both experiments, replacement of the ¹H NMR signals of **1** by those of **4** (R = Ph) was complete and quantitative after several hours upon reaction at either room temperature or 45 °C. However, in neither the former experiment, probed by ²H NMR, nor the latter, probed by ¹H NMR, was there any evidence for deuterium "wash-in" or "wash-out", respectively, in the resonances assigned to the methyl groups on the trimethylphosphine ligand. An attempted preparation of the [CpIr(PMe₃)(CH₃)(OTf)] complex **5** in CD₂Cl₂ resulted only in the rapid darkening of the solution and the production of uncharacterizable products. One presumes that the qualitatively greater reactivity of the Cp versus Cp*-substituted complex leads to reaction with the solvent and/or decomposition.

Because a small amount of reaction of **6** with CH₂Cl₂ could be seen in the gas phase under certain conditions, it was thought that use of a more inert solvent might be advisable. Accordingly, treatment of the [CpIr(PMe₃)(CH₃)(I)] complex with AgOTf in purified C₆F₆ in the presence of C₆D₆ led to the disappearance of the ¹H NMR signals for starting material, and the appearance of a red precipitate that unfortunately exhibited such low solubility in C₆F₆ that no ¹H NMR spectrum could be seen. When the precipitate was collected and redissolved in acetonitrile, the electrospray mass spectrum showed [CpIr-(PMe₃)(CH₃)(CH₃CN)]⁺. (We find that acetonitrile traps any of the 16-e⁻ complexes and stops any further reactions.) Evidently, ionization of the CpIr(PMe₃)(CH₃)(I) to the triflate salt had occurred, but poor solubility of the complex led to precipitation before any reaction could occur. On the other hand, reaction of ~7 mg of CpIr(PMe₃)(CH₃)(Cl) in 1.5 mL of C₆F₆ with 1 equiv of Ag(O₃SC₈F₁₇), instead of AgOTf, led to the appearance of the AgCl precipitate above which stood a supernatant solution, which was filtered and added rapidly to a 3-fold excess of CD₂Cl₂/C₆D₆ (30:1 v/v) at room temperature. The ¹H NMR spectrum showed CH₄ and the appearance of three distinct species (by both the Cp and the −PMe₃ resonances) whose relative amounts changed over a period of a day. Periodic quenches of an aliquot with acetonitrile, followed by electrospray mass spectrometry, also showed the formation of three ionic complexes: the expected [CpIr(PMe₃)(CH₃)(CH₃-CN)]⁺ and [CpIr(PMe₃)(C₆H₅)(CH₃CN)]⁺ complexes, and a doubly-charged dimeric species,[31] ([CpIr(PMe₂)(CH₂)(CH₃-CN)]⁺)₂, of as yet undetermined structure. After 12 h at room temperature, the reaction was complete, with only the latter two complexes remaining. When the experiment was done in the

(32) Care must be taken that the C₆F₆ and C₅F₅N solvents are freshly distilled from CaH to remove all traces of protic acid, presumably HF. We find the CpIr(PMe₃)(CH₃)(OTf) complex to be very susceptible to protonation and subsequent loss of methane.

(33) An intramolecular addition would simply be the **6** → **7** reaction, and would produce CH₃D. An intermolecular addition to a C−D bond in the deuterated trimethylphosphine ligand, done twice, would be one way to the dimeric complex of ref 31, and would also produce CH₃D.

Scheme 4
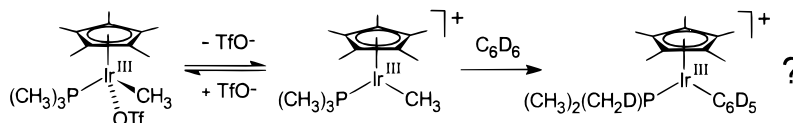
absence of benzene, only the first and third complexes were produced. The same chemistry is also observed when CpIr-(PMe$_3$)(CH$_3$)(Cl) is treated with AgOTf in perfluoropyridine. In that case, the AgOTf was dissolved in C$_5$F$_5$N prior to addition to a solution of the iridium complex. Treatment of CpIr(PMe$_3$-d_9)(CH$_3$)(Cl) in an identical fashion gave the corresponding CpIr(PMe$_3$-d_9)(CH$_3$)(OTf) complex in C$_5$F$_5$N solution, which again slowly dimerized over a period of 12 h in the absence of hydrocarbon traps. Methane[32] produced in the reaction without added hydrocarbon was clearly shown by ^{1}H NMR to be CH$_3$D, although it is not clear whether the deuterium incorporation came from an intra- or intermolecular addition to the deuterated trimethylphosphine ligand.[33] Lastly, we find that, with C$_6$D$_6$ present in the C$_5$F$_5$N solution as the complex is prepared, CpIr-(PMe$_3$)(CH$_3$)(OTf) reacts with the evolution of both CH$_4$ and CH$_3$D, although again, the presence of significant amounts of the dimeric complex makes it difficult to identify the reaction producing CH$_4$. The electrospray mass spectrum of the [CpIr(PMe$_3$)(Ph)(CH$_3$CN)]$^+$ product in the reaction with C$_6$D$_6$, after acetonitrile quench, showed five deuteriums rather than six, making it clear that if **6** and **7** were both present, then all of the **7** would have had to have ended up in the dimer rather than in the adduct with benzene.

The geometries and relative energies of several of the important organometallic structures, computed by the *ab initio* methods described above, are shown in Figures 8–10. For all three structures, the structures were verified to be minima by computation of the frequencies, which are tabulated in the Supporting Information along with the Cartesian coordinates of each atom. If one draws a "bond" from the iridium atom in **6** or **7** to the center of the Cp ring, then the sum of C–Ir–P, Cp–Ir–P, and Cp–Ir–C angles is a measure of the "planarity" at the iridium center. In Figure 8, the view of **6** is chosen to emphasize the nearly "planar" arrangement of ligands around the metal (sum of angles ∼358°). Similarly, the view of **7** in Figure 9 shows that the metal is now "pyramidalized" (sum of angles ∼339°). While a definitive judgment will require a more thorough computational study, one can suspect that the differences in reactivity between **6** and **7** could stem from a combination of better steric access to the metal in **7** and electronic differences imposed by the different geometry about the iridium center. A full exploration of the hypersurface
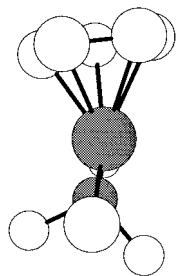
connecting the various energy minima is beyond the scope of the present report and will be the subject of future investigations. Looking at the DFT results, one sees that the relative energies of **6** and **7** are not too well described, with the cyclometalated complex **7** (plus CH$_4$) predicted to lie 26 kcal/mol above the open structure **6**. As a comparison, the CID threshold experiment places an upper-bound on the energy difference of 13.6 kcal/mol. Three stationary points were found with an Ir(V) structure **9** containing the same three-membered ring, as well as Ir–CH$_3$ and Ir–H bonds, designated **9** with *cis-anti*, *cis-syn*, and *trans* configuration of the Ir–CH$_3$ and Ir–H bonds (Scheme 5). Although the two *cis* structures are almost identical in energy (within 1 kcal/mol), with the *trans* structure 24 kcal/mol higher in energy, only the *cis-anti* (on geometrical grounds) structure can be the first-formed intermediate (or transition-state)
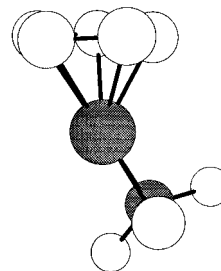
Figure 9. Computed (DFT with B3LYP functional and LANL2DZ basis set) structure of **7** viewed along the plane formed by the C–Ir–P atoms (Ir–C bond in front) to emphasize the near "pyramidalization" at the central iridium atom. The hydrogen atoms are not shown. Important bond lengths: Ir–Cp (center of ring) 1.93 Å, Ir–C 2.10 Å, Ir–P 2.41 Å, P–C 1.88 and 1.87 Å (shorter bond on "concave" side). Important bond angles: C–Ir–P 47.56°, Cp–Ir–P 147.06°, Cp–Ir–C 144.25°. Note the sum of the bond angles about the central iridium atom is 338.87°. Total energy: −423.56517 hartrees for **7** and −40.51448 hartrees for methane.

Figure 8. Computed (DFT with B3LYP functional and LANL2DZ basis set) structure of **6** viewed along the plane formed by the C–Ir–P atoms (Ir–C bond in front) to emphasize the near "planarity" at the central iridium atom. The hydrogen atoms are not shown. Important bond lengths: Ir–Cp (center of ring) 1.95 Å, Ir–C 2.05 Å, Ir–P 2.41 Å, P–C 1.88 Å (for all three methyls). Important bond angles: C–Ir–P 89.96°, Cp–Ir–P 134.15°, Cp–Ir–C 133.54°. Note the sum of the bond angles about the central iridium atom is 357.65°. Total energy: −464.12127 hartrees.

Figure 10. Computed (DFT with B3LYP functional and LANL2DZ basis set) structure of *cis-anti*-**9**, the putative product of an intramolecular oxidative addition by **6**, viewed along the plane formed by the C(ring)–Ir–P atoms (Ir–C bond in front) to show the relationship of the hydrido and methyl ligands to the ring. Only the Ir–H hydrogen atom is shown. Important bond lengths: Ir–Cp (center of ring) 2.02 Å, Ir–C(ring) 2.18 Å, Ir–C(methyl) 2.15 Å, Ir–P 2.41 Å, P–C 1.87 Å (for both methyls), Ir–H 1.57 Å. Important bond angles: C(ring)–Ir–P 46.16°, Cp–Ir–P 136.20°, Cp–Ir–C(ring) 123.69°, Cp–Ir–C(methyl) 116.41°, Cp–Ir–H 123.85°, C(ring)–Ir–C(methyl) 119.70°, C(ring)–Ir–H 77.32°, P–Ir–H 97.29°, P–Ir–C(methyl) 86.77°, C(methyl)–Ir–H 73.95°. Note the two important distances C(ring)–H and C(methyl)–H are 2.39 and 2.29 Å, respectively. Total energy: −464.09308 hartrees for *cis-anti*-**9**. *cis-syn*- and *trans*-**9** lie at −464.09426 and −464.05455 hartrees, respectively.

Scheme 5

cis-anti **9**   *cis*-syn **9**   *trans* **9**
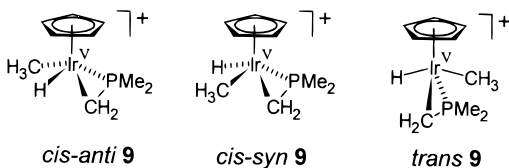
for a hypothetical reaction from **6** to **7** via a discrete Ir(V) species. The DFT calculations place *cis*-anti-**9** approximately 18 kcal/mol above **6**. While the numbers, taken literally, place *cis*-anti-**9** below (**7** + CH$_4$), the disagreement with experiment (see below) on the **6** versus (**7** + CH$_4$) energy difference, combined with the well-known problems in computing bond energies (BSSE, size-consistency, etc.), means that one can only say with certainty that both **7** and *cis*-anti-**9** are energetically accessible structures that could plausibly be important in the C−H activation chemistry of **6**.

Discussion

At the nonquantitative level, the mass spectrometric observation of organometallic complexes, including reactive intermediates, is straightforward,[34−37] and qualitative observation of collision-induced reductive elimination from electrosprayed Pd-(IV) complexes, for example, has even been reported.[38] The range of organometallic systems for which electrospray mass spectrometry can been done suggests broad applicability as both an analytical and mechanistic tool. While there have been CID threshold measurements on other organometallic species,[39,40] the present work represents the first application of the method to organometallic complexes that appear as reagents or catalysts in solution-phase chemistry.

The gas-phase reactions of the cationic Ir(III) complexes, as observed in the mass spectra, clearly point to a previously unreported mechanism for their observed σ-bond metathesis reactions. Previous discussions had considered a two-step mechanism involving intermolecular oxidative addition of either **2** or **6** to the C−H bond of an alkane or arene producing an Ir(V) intermediate, followed by reductive elimination of methane, or a concerted σ-bond metathesis reaction similar to that seen in early transition metals. The electrospray mass spectra show another mechanism involving initial elimination of methane, followed by addition to an alkane or arene, with all detected reactive intermediates retaining a formal +3 oxidation state.

Structural Assignment. The structures of the intermediate species, **3** and **7**, are assigned on the basis of literature precedent, *ab initio* calculations, and the present experimental observations. The masses of **3** and **7**, as well as isotopic labeling experiments, strongly suggest a cyclic structure with cyclometalation occurring on the phosphine and not the Cp or Cp* ligand. Numerous examples of transition metal complexes with the η^2-CH$_2$PMe$_3$ ligand have been reported and characterized by X-ray crystallography.[41−44] For at least one of the iridium complexes from the

Scheme 6
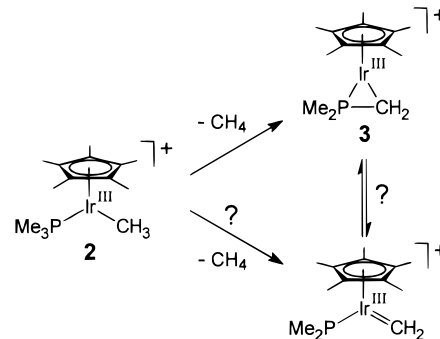
literature, an alternative structure, an isomeric L$_3$Ir(PR$_2$)(CH$_3$) phosphido complex, has been shown to rearrange irreversibly to L$_3$Ir(H)(η^2-CH$_2$PMe$_3$),[43] which indicates at least some relative stability. Furthermore, a reversible intramolecular C−H insertion reaction on the trialkylphosphine ligand has also been reported for several complexes of iron, nickel, manganese, rhenium, ruthenium, and osmium,[45] with the equilibrium lying toward the cyclometalated product. The cyclometalation reactions of **2** and **6** differ from these primarily in the concomitant loss of methane, removing any possibility of reversibility. The observed threshold for methane loss from **6** of 13.6 kcal/mol is also consistent with the structural assignment. The facile addition of **7** to alkanes and arenes indicates that the reactions of **7** occur over a rather low barrier. Accordingly, one would expect the heat of formation of (**7** + CH$_4$) to be something like 10 kcal/mol above that of **6**. The principal difference between the two complexes is just ring strain, with a small contribution from the difference between the C−H bond strength in methane and that in the methyl group on the phosphine ligand. A difference of ∼10 kcal/mol is just about what one would expect.

An alternative structural possibility for **7** was considered, and then excluded by the experimental evidence. A methylidene complex bearing a phosphido ligand, isomeric with **3** or **7**, differs from the cyclometalated structures primarily in the P−C distance. A number of methylidene complexes of iridium have been reported.[46] Furthermore, precedent for conversion of C−H activation products to the Fischer carbene complexes has been found for cationic Ir(III)[47] and Pt(II)[7] complexes. One can therefore envision a case where the carbene complex is formed from **3** or **7**. One can even consider the possibility that the carbene complex lies on the reaction coordinate from **2** or **6** as the first-formed reactive intermediate. The latter possibility can be excluded in the gas-phase reaction, **2** → **3** + CH$_4$. Entries 21 and 22 in Table 1 clearly indicate that [Cp*Ir(PMe$_3$-d$_9$)-

(34) Colton, R.; Traeger, J. C. *Inorg. Chim. Acta* **1992**, *201*, 153. Colton, R.; D'Agostino, A.; Traeger, J. C. *Mass Spectrom. Rev.* **1996**, *14*, 79.

(35) Kane-Maguire, L. A. P.; Kanitz, R.; Sheil, M. M. *J. Organomet. Chem.* **1995**, *486*, 243.

(36) Lipshutz, B. H.; Stevens, K. L.; James, B.; Pavlovich, J. G.; Snyder, J. P. *J. Am. Chem. Soc.* **1996**, *118*, 6796.

(37) Spence, T. G.; Burns, T. D.; Posey, L. A. *J. Phys. Chem. A* **1997**, *101*, 139.

(38) Canty, A. J.; Traill, P. R.; Colton, R.; Thomas, I. M. *Inorg. Chim. Acta* **1993**, *210*, 91.

(39) Freiser, B. S. *Organometallic Ion Chemistry*; Kluwer: Dordrecht, 1996.

(40) Armentrout, P. B. *Acc. Chem. Res.* **1995**, *28*, 430.

(41) Lindner, E.; Neese, P.; Hiller, W.; Fawzi, R. *Organometallics* **1986**, *5*, 2030.

(42) Al-Jibori, S.; Crocker, C.; McDonald, W. S.; Shaw, B. L. *J. Chem. Soc., Dalton Trans.* **1981**, 1572.

(43) Fryzuk, M. D.; Joshi, K. *J. Am. Chem. Soc.* **1989**, *111*, 4498. Fryzuk, M. D.; Joshi, K.; Chadha, R. K.; Rettig, S. J. *J. Am. Chem. Soc.* **1991**, *113*, 8724.

(44) Hester, D. M.; Yang, G. K. *Organometallics* **1991**, *10*, 369.

(45) Karsch, H. H.; Klein, H.-F.; Schmidbauer, H. *Angew. Chem.* **1975**, *87*, 630. Rathke, J. W.; Muertterties, E. L. *J. Am. Chem. Soc.* **1975**, *97*, 3272. Klein, H.-F. *Angew. Chem., Int. Ed. Engl.* **1980**, *19*, 362. Morvillo, A.; Turco, A. *J. Organomet. Chem.* **1981**, *208*, 103. Werner, H.; Werner, R. *J. Organomet. Chem.* **1981**, *209*, C60. Lindner, E.; Starz, K. A.; Eberle, H. J.; Hiller, W. *Chem. Ber.* **1983**, *116*, 1209. Lindner, E.; Küster, E. U.; Hiller, W.; Fawzi, R. *Chem. Ber.* **1984**, *117*, 127. Karsch, H. H. *Chem. Ber.* **1984**, *117*, 3123. Bergman, R. G.; Seidler, P. F.; Wenzel, T. T. *J. Am. Chem. Soc.* **1985**, *107*, 4358. Wenzel, T. T.; Bergman, R. G. *J. Am. Chem. Soc.* **1986**, *108*, 4856. Hartwig, J. F.; Andersen, R. A.; Bergman, R. G. *J. Am. Chem. Soc.* **1991**, *113*, 6492.

(46) Clark, G. R.; Roper, W. R.; Wright, A. H. *J. Organomet. Chem.* **1984**, *273*, C17. Fryzuk, M. D.; McNeil, P. A.; Rettig, S. J. *J. Am. Chem. Soc.* **1985**, *107*, 6708. Klein, D. P.; Bergman, R. G. *J. Am. Chem. Soc.* **1989**, *111*, 3079. Fryzuk, M. D.; Gao, X.; Joshi, K.; McNeil, P. A.; Massey, R. L. *J. Am. Chem. Soc.* **1993**, *115*, 10581.

(47) Lücke, H. F.; Arndtsen, B. A.; Burger, P.; Bergman, R. G. *J. Am. Chem. Soc.* **1996**, *118*, 2517.

Scheme 7

$(CH_3)]^+$ loses CH_3D upon collisional activation, indicating that the carbon leaving as methane came from the methyl group directly attached to the metal. If the carbene complex were to be the first-formed intermediate, one would expect the departing carbon to come from one of the methyls in the trimethylphosphine ligand, giving loss of CHD_3 instead. The characteristic C−H activation chemistry we report is moreover inconsistent with the reactions reported for the known methylidene complexes,[46] meaning, that if there were to be interconversion between **3** or **7** and the corresponding carbene complexes, it would be a nonproductive equilibrium lying off of the main reaction pathway.

The experiment listed as entry 12 in Table 1 was done to check the structure of **6**. One could have imagined that **9**, with the same mass as **6**, could be the species actually prepared by electrospray ionization of **5**. While not yet definitive, the experiment is strongly suggestive that the ion is the 16-electron complex **6** rather than the 18-electron complex **9**. Entry 12 corresponds to a daughter-ion experiment in which thermalized ions with the mass corresponding to **6** are selected, and collided with acetonitrile or CO in O2 at very low collision energies. In this instance, the pressure of acetonitrile vapor or CO in O2 was set to correspond to approximately 100 collisions by the average ion before it exits into the mass analyzer. Nearly all molecules of **6** pick up an additional acetonitrile or CO ligand under these conditions. The observation of a very minor mass peak due to **7** indicates that there is sufficient energy in the collisions to induce a small amount of cleavage of CH_4. A larger (but still smaller than the peaks due to **6** and (**6** + acetonitrile)) peak due to (**7** + acetonitrile) indicates that **7** also picks up a 2-electron ligand. Not all molecules of the unambiguously 16-electron complex **7** pick up an acetonitrile or CO despite multiple collisions because, presumably, the reactive cross section in the collision is smaller than the hard-sphere cross section. Taken altogether, these observations strongly suggest that the ion with the mass of **6** is indeed the 16-electron structure **6** and not the 18-electron structure **9**. A control experiment whereby the unambiguously 18-electron complex **5** (L = CH_3CN) is tested under the same conditions shows no pickup of an additional ligand. This rules out the formation of electrostatically bound ion−dipole complexes as the explanation for the acetonitrile or CO "trapping" results above.

Comparison of the Cp and Cp* Series of Complexes. The difference in the extent of isotopic exchange between the trimethylphosphine and the phenyl ligand upon CID of **4** versus **8** (R = Ph) very likely comes from a general feature of ion−molecule reactions. In the gas phase, ion−molecule reactions proceed through a charge-dipole or charge-induced dipole complex bound by anywhere from a few to several kilocalories per mole relative to the separated molecules. The non-negligible attractive potential is relatively long ranged, i.e. $1/r^2$ falloff with

distance for a charge-dipole interaction and $1/r^4$ for a charge-induced dipole interaction, and amounts to a potential well in which the reacting partners of a bimolecular ion−molecule reaction are trapped prior to reaction (Scheme 7).[48] In the absence of subsequent thermalizing collisions, the charge-dipole or charge-induced dipole interaction can provide the energy needed to surmount an activation barrier for the trapped reactants as long as the transition state is not substantially higher in energy than the separated reactants. Neglecting for the moment any other shallow minima that may lie on the reaction coordinate, the potential energy diagram above rationalizes the very high reactivity in the reaction of **7** with benzene, as well as the extensive isotopic exchange between the trimethylphosphine and the hydrocarbon ligand. By microscopic reversibility, CID of **8** (R = Ph) to produce **7** and benzene should go through the same charge-induced dipole complex. As long as the transition state for the conversion of the complex to the adduct lies below the asymptotic limit for separate molecules, the first step of the dissociation should be reversible, leading to the extensive isotopic scrambling. Going to the Cp* series, the potential energy diagram is drawn with the same energy difference between the two minima, and the same activation barrier between them (for argument's sake), but a shallower well for the complex relative to the separated molecules. One would justify this change by invoking both the increased steric bulk of the Cp* ligand and the greater degree of charge-delocalization in **3** (relative to **7**) as factors making the charge-induced dipole interaction less stabilizing. Having lowered the asymptote relative to the two minima and the transition state for reaction, a small activation energy now appears for the bimolecular gas-phase reaction. It may or may not be possible to measure the resulting barrier to the **3** + benzene addition reaction if it is only few kilocalories per mole, but importantly, the reverse reaction, CID of **4** (R = Ph), would now proceed without reversiblity in the first step of the dissociation, limiting the isotopic exchange to zero or one label.

One should note that the reaction of **7** with CH_4 (daughter-ion mode, mass-selected **7**, collision in O2, not reported in Table 1 because the extent of reaction was very small or zero) must undoubtedly follow a potential energy diagram similar to that shown in Scheme 8 for **3** and benzene, i.e. the transition state for the interconversion between the two minima must lie above the separated molecules. Presumably, the small size and consequent low polarizability of CH_4 leads to an even less stabilizing charge-induced dipole interaction. Accordingly, even complex **7** reacts poorly, if at all, with methane. The CID

(48) Farneth, W. E.; Brauman, J. I. *J. Am. Chem. Soc.* **1976**, *98*, 7891. Olmstead, W. N.; Brauman, J. I. *J. Am. Chem. Soc.* **1977**, *99*, 4219. Asubiojo, O. I.; Brauman, J. I. *J. Am. Chem. Soc.* **1979**, *101*, 3715. Pellerite, M. J.; Brauman, J. I. *J. Am. Chem. Soc.* **1980**, *102*, 5993. Sharma, S.; Kebarle, P. *J. Am. Chem. Soc.* **1982**, *104*, 19. Caldwell, G.; Magnera, T. F.; Kebarle, P. *J. Am. Chem. Soc.* **1984**, *106*, 959. McMahon, T. B.; Heinis, T.; Nicol, G.; Hovey, J. K.; Kebarle, P. *J. Am. Chem. Soc.* **1988**, *110*, 7951.

Scheme 8
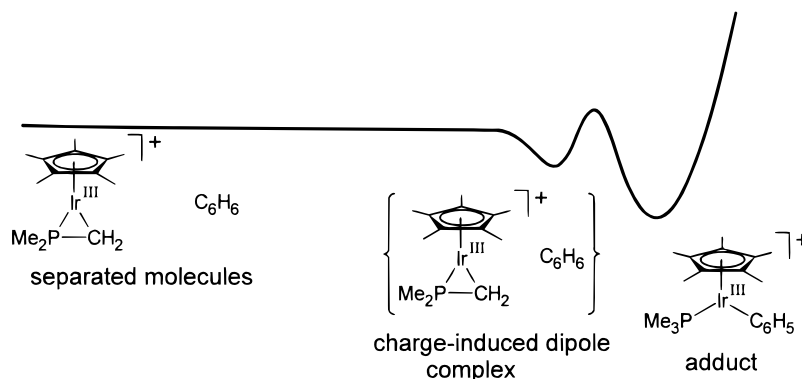
threshold for the reverse reaction, loss of methane from **6**, is therefore interpreted as a $\Delta G^{\ddagger}$ rather than a ΔG for the reaction. Similarly, one can postulate that the difference between **3** and **7** in their reactions with cyclohexane may stem from this same model. The extra methyl groups in **3** may force the intermediate complex in the addition reaction of **3** and cyclohexane to adopt a geometry where the two molecules are farther apart on average than they are in the complex of **7** and cyclohexane. The potential surfaces for addition of **7** and **3** to cyclohexane would show the same differences as between Scheme 7 and Scheme 8 except that, in the case of reaction with cyclohexane, the activation barrier in Scheme 8 would be high enough to stop reaction at all accessible collision energies. In short, benzene is highly reactive with the cationic metallaphosphacyclopropanes because, with its large π-system, it is highly polarizable. Pentane reacts because the 1° C−H bonds at its termini can approach even a sterically hindered ion. Cyclohexane, with its 2° C−H bonds, cannot approach as closely, so the reaction is worse. Lastly, methane, although it is small, is the least polarizable of the aliphatic hydrocarbons, and therefore forms only weakly-bound charge-induced dipole complexes, giving the lowest reactivity.

One last comment derived from the qualitative potential surfaces needs to be made. In solution, the dielectric screening of electrostatic interactions reduces the charge-dipole or charge-induced dipole interaction between the two reactant molecules to near zero until the reacting species are practically in contact. The effect on the qualitative potential surface would be to pull the asymptote representing separated molecules down relative to the electrostatic complex until there is only a very shallow minimum (which presumably is the physical basis for a cage effect in solution-phase reactions). Accordingly, isotopic exchange between the trimethylphosphine and a phenyl ligand in *both* the Cp and Cp* series of compounds should involve no more than one labeled atom per event, when the reaction is performed in solution. Of course, multiple exchange would still be possible if a reversible solution-phase reaction were to occur repeatedly, but that is a trivial case.

**Comparison of the Gas-Phase to Solution-Phase Results.** The results are unambiguous that, in the gas-phase, loss of methane precedes reaction with C−H bonds for both the Cp and Cp*-substituted complexes. The solution-phase results for [Cp*Ir(PMe$_3$)(CH$_3$)(OTf)] are equally compelling in that the absence of isotopic exchange between the trimethylphoshine ligand and the incoming hydrocarbon rules out the participation of an intermediate of structure **3**. We have also been recently apprised of unpublished results from the Bergman group,[49]

which also suggest that the mechanism we observe in the gas phase does not occur to a significant extent in solution for **1**.

We can postulate an explanation for the difference between the gas-phase and solution-phase results. A concerted σ-bond metathesis was originally offered as an alternative to the more conventional oxidative addition/reductive elimination mechanism for the observed C−H activation chemistry of the Ir(III) complexes because it was thought that an electron-deficient Ir-(III) might find it unfavorable to proceed via an even more electron-deficient Ir(V) intermediate.[2] A subsequent search for an accessible transition state for the concerted mechanism by *ab initio* computational techniques was unsuccessful, leading to the conclusion that the reaction proceeded by addition−elimination after all.[6] The mechanism found in the present gas-phase work was not considered in that study, but nevertheless could have provided yet another alternative to the conventional oxidative addition/reductive elimination mechanism that could again avoid the Ir(V) intermediate if the methane loss and C−H activation steps each were to proceed concertedly with the formation or cleavage of the three-membered ring. If one presumes that both an addition−elimination and an elimination−addition mechanism were to be plausible, and, furthermore, that they proceed through transition states that are not too different in energy, then electron donation by solvent or simple electrostatic stabilization of charged species in a dielectric continuum could tip the balance in favor of a route through an Ir(V) intermediate. External stabilization of an electron-deficient species is absent, of course, in the gas-phase experiments. Our preliminary solution-phase results for CpIr(PMe$_3$)(CH$_3$)(OTf) in C$_5$F$_5$N solution indicate that the more electron-deficient complexes undergo some different chemistry. While we could exclude isotope exchange between the phosphine ligand and the incoming hydrocarbon in reactions of CpIr(PMe$_3$)(CH$_3$)-(OTf) with C$_6$D$_6$, the observation of CH$_4$ evolution associated with dimer formation indicates a mechanism involving an addition to the C−H bond on the trimethylphosphine. What is as yet unclear is whether the reaction is intra- or intermolecular. In the former case, intramolecular insertion would produce **7**, which presumably then dimerizes or reacts with another molecule of uncyclized complex. In the latter case, one could have an ordinary oxidative addition/reductive elimination sequence, done twice, which would give the same CH$_4$ as well as the same dimeric complex. The experiments to date do not distinguish between the two possibilities, although it would be odd for an intermolecular addition to occur to the exclusion of the intramolecular version. While a definitive conclusion will require much further work, the preliminary results suggest that the more electron deficient Cp-substituted complexes may be reacting in solution, at least in part, by the same elimination−addition mechanism seen in the gas phase. The proposition can be tested in two ways. By rendering the complexes even more

(49) The reaction of **1** and benzene or deuteriobenzene in solution shows a primary deuterium kinetic of $k_H/k_D \sim 4$, which can be interpreted to mean that C−H cleavage on the arene occurs in the rate-determining step. R. G. Bergman, private communication.

Scheme 9
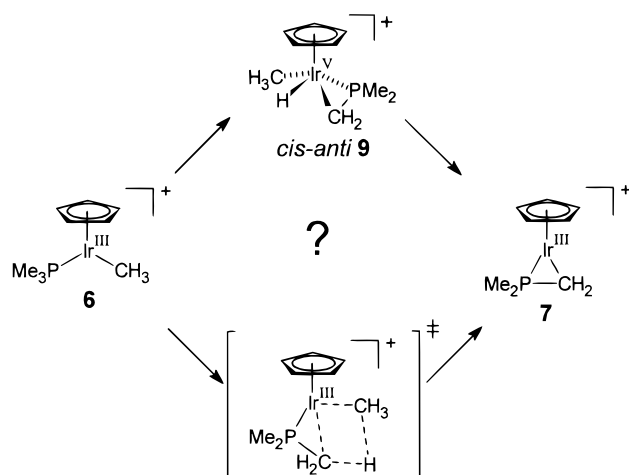
electron deficient through use of functionalized phosphines, the oxidative addition through an Ir(V) intermediate could be increasingly disfavored, allowing competing mechanisms to appear. A more direct approach is the independent syntheses of **3** and **7**, and an investigation of their reactivity in the gas phase and solution. Both experiments are underway.

Mechanism of Methane Loss. Presumably, the preference for **2** and **6** to react in the gas phase via the elimination−addition mechanism comes from the aforementioned reluctance of the formal Ir(III) center to go to the requisite Ir(V) of an oxidative addition product. The claim really only pushes the question back one step, though. In going from **2** to **3**, or **6** to **7**, one can again imagine a two-step mechanism involving intramolecular oxidative addition through an intermediate *cis-anti*-**9**, followed by reductive elimination of CH_4, or a concerted mechanism through a four-center transition state. The absence of any C−H activation chemistry by the $CpFe(CO)(\eta^2\text{-}CH_2PEt_2)$ complex[44] (an 18-e$^-$ complex) could be interpreted to mean that the metal center is involved in an addition reaction. Nevertheless, the present experimental results do not distinguish decisively between the two possibilities shown in Scheme 9. The *ab initio* calculations do find *cis-anti*-**9** to be a minimum. Of special interest are the H−Ir, H−CH_2, and H−CH_3 distances in that structure, which are computed to be 1.57, 2.39, and 2.29 Å. Comparing these to the H−Ir and H−CH_3 distances in the computed structure of the $[CpIr^V(PH_3)(CH_3)_2(H)]^+$ intermediate by Hall and co-workers,[6] one sees that the present numbers more closely resemble the 1.567 and 2.194 Å for a product of an oxidative addition than the 1.611 and 1.535 Å for a transition state. Computed to lie 18 kcal/mol above **6**, *cis-anti*-**9** is predicted to be lower in energy than the sum of the computed energies for **7** and methane. However, given the basis set superposition error, size consistency, etc. problems at this level of theory, and given that the calculations are only single points and not a complete surface, one still cannot judge with certainty whether or not *cis-anti*-**9** is on the reaction coordinate from **6** to **7**. On thermochemical grounds, however, one can place real limits on *cis-anti*-**9**, if it were to be an intermediate in the reaction. The structural arguments cited earlier can be interpreted to mean that we see no evidence for an Ir(V) structure

in an experiment designed to produce it (if it were an intermediate), which means that, in accordance with the prediction from theory, one would have to place *cis-anti*-**9** energetically above **6** by more than a few kilocalories per mole. Meanwhile, we also have the experimentally determined activation energy for the loss of CH_4 from **6** at only 13 kcal which would be a rigorous upper-bound on the amount above **6** that *cis-anti*-**9** could lie if it were on the reaction coordinate. One can be reasonably certain in concluding, therefore, that if *cis-anti*-**9** were to be an intermediate in the reaction **6** → **7** + CH_4, it would have to reside in, at best, a shallow minimum no more than a few kilocalories per mole deep.

Conclusions

Electrospray ionization tandem mass spectrometry, in conjunction with solution-phase experiments and *ab initio* calculations, is a new approach to the study of organometallic reactions and reactive intermediates. Both the similarities and the differences between the observed gas-phase and solution-phase chemistry hold information useful to the dissection of complex reaction pathways. In the particular case of C−H activation by cationic Ir(III) complexes, a novel mechanism involving metallaphosphacyclopropane intermediates has been found. The balance favoring this mechanism over competing mechanisms not involving cyclometalation depends on the presence or absence of solvent, and may be adjustable by perturbations in structure or surroundings. The multiplicity of competing mechanisms and energetically similar structural types in organometallic chemistry has often been blamed for the poor state of mechanistic understanding in the field, but with the introduction of new, powerful physical techniques, this problem can potentially become an asset. We see that changes in mechanism can be induced by small changes in the molecule or its surroundings, which if properly understood can then be used to fine-tune reactivity rationally. This possibility will be tested in subsequent investigations.

Supporting Information Available: Geometries, absolute energies, and the frequencies for **6, 7**, and **9** from the *ab initio* calculations with the HF and DFT methods, as well as the synthetic details and physical characterization of the complexes in this study (10 pages). See any current masthead page for ordering and Internet access instructions.

JA970995U